Effects of Stores on Aircraft Structure

Wolfgang G. LUBER
wgl-dynamics
81735 Munich
GERMANY
+49-172 832 9241

wolfgang.luber@live.de

ABSTRACT

The approach to prove structural integrity of military combat aircraft with external stores focus on the understanding of the fundamental structural dynamics mechanisms involved and the identification of boundaries for all potential store loading up to the design limit of the aircraft.

A finite element model is required which will be updated with ground and flight test results. The basic for the analytical investigation can be a coarse grid model which is derived from fine finite element component models, assembled to a complete aircraft model. The advantage of using the fine static grid model as basic model is that in case of refinement all used models can be updated in one step. From selected assumed mode a set of generalized unsteady aerodynamic matrices will be calculated. To analyze real conditions, aerodynamic interference of different surfaces is investigated. The analytical calculations were verified by low speed wind tunnel tests and flight test. The main flight tests are flutter, structural coupling, and vibration and loads survey. Different excitation methods and maneuvers were used to excite the aircraft in a symmetric or antisymmetric case.

1.0 INTRODUCTION

The layout of military aircraft structures is strongly influenced by dynamic loads from the early development phase onwards up to final design and clearance phase. Different dynamic loads have to be considered, namely dynamic gust loads, buffet loads on wing, fin, fuselage also buffet loads from airbrakes, cavities and blisters, gunfire loads mainly at attachment frames and panels, Hammershock loads for air intake, bird strike and ammunition impact, acoustic loads for outer air intake and missile bays. Also dynamic loads from landing, jettison, brake chute and rough runway induced loads as well as wake induced loads may be designing. Dynamic loads resulting from flight test excitation like bunker input, stick jerks and control surface sweeps also have to be considered.

For some of the designing dynamic loads examples are given to explain their derivation and significance both for design of aircraft structural parts and related clearance aspects. Methods to derive dynamic design loads for different application by using analytical and experimental tools will be discussed.

Validation methods for various design loads using dynamic model test results, wind tunnel model and flight test results are mentioned.

Main purpose of this presentation is to indicate where dynamic loads would be dimensioning structures of high performance combat airplanes with external stores and how to approach the problem of integrating all aspects into an optimum design.

Flutter certification of an aircraft which is required to carry many different types of external stores is general a highly complex and tedious task. The most aircraft operate in the transonic flight regime and carry large under wing stores.

In aircraft development a limited number of specific stores (baseline configuration) and of additional store loading (key-configuration) will be certificate to the aircraft weapon system specification. At the ends of the program development phase or when the Aircraft is in service an additional loading (follow-on stores) must be cleared with minimally engineering resources and in the presence of minimum cost normally in a constraint time.

The table 1 below shows the different source of Loading and the affected components. The component affected is divided into external Store itself and in the Aircraft structure. As we can see most of the different loadings influence both the Aircraft structure and the external store structure and both together. In this report mainly the loading cases explained for the consideration of the Aircraft with external stores. In case of store release the aircraft will have in some cases an asymmetric weapon carriage. For landing impact asymmetric landing with or without cross wind is in most cases a real challenge. The Structural Dynamics department must analyse each of this cases for save handling of the aircraft on ground and airborne.

Table 1: Source of Loading vs. component affected.

	Store			Aircraft Structure				
Components affected / Source of Loading	Store	Pylon	Attachment	Wing	Fin	Foreplane, Tailplane	Fuselage	Crew
Atmospheric Turbulence Gust	X	X	X	X	X	X	X	X
Buffet / Buffeting / Buzz	X	X	X	X	X	X	X	X
Landing impact, Ground Operations	X	X	X	X	X	X	X	X
Birdstrike	X	X	X	X	X	X	X	
Store Release & Jettison		X	X	X			X	
Missile Firing		X	X	X				

2.0 EXAMPLES OF AIRCRAFT RESPONSE PREDICTION

Some typical results of gust response calculations on a flexible aircraft investigation are listed here in order to demonstrate the importance of arising problems.

The investigated aircraft is a delta canard configuration with wing tip mounted stores. The first example shall illustrate the prediction of vibration levels on external stores and resulting dynamic wing loads due to discrete gusts, Figure 1. The total aircraft configuration is idealized for unsteady aerodynamic force calculation by the grid shown in Figure 2.

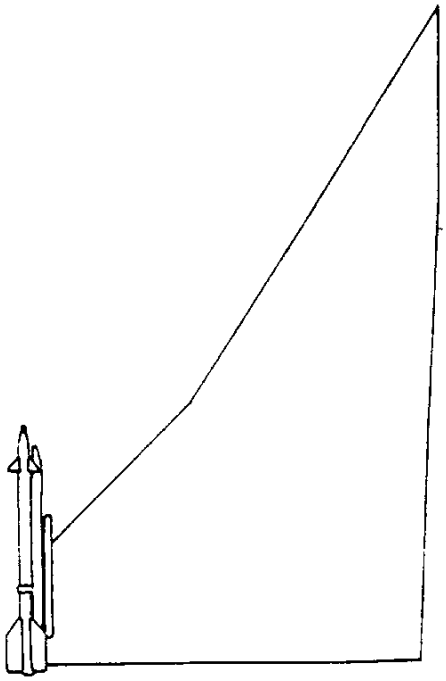

Figure 1: Wing with Tip Mounted Missile.

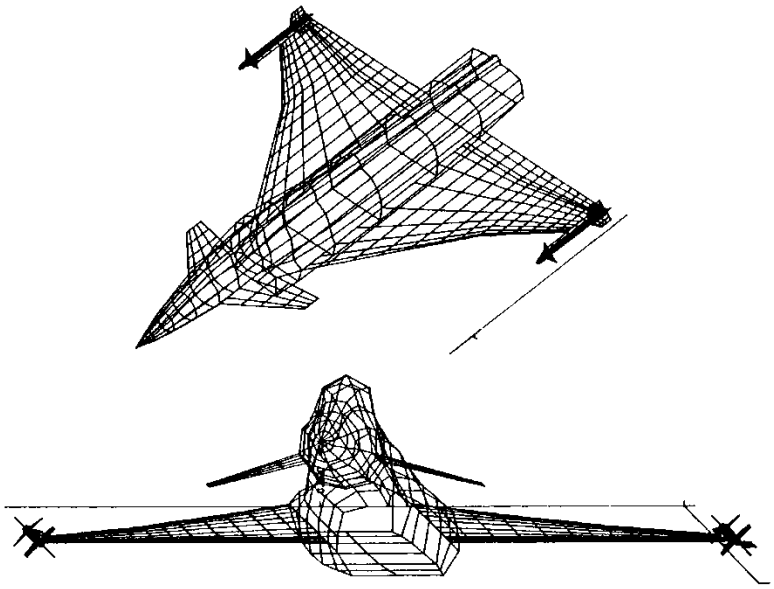

Figure 2: Aerodynamic Grid (Idealization).

The unsteady aerodynamic derivatives and generalized forces together with load distributions on subcomponents are calculated with the programs for the degrees of freedom aircraft angle of attack, rotation around centre of gravity, canard deflection, flap deflection and wing elastic normal modes shown in Figure 3.

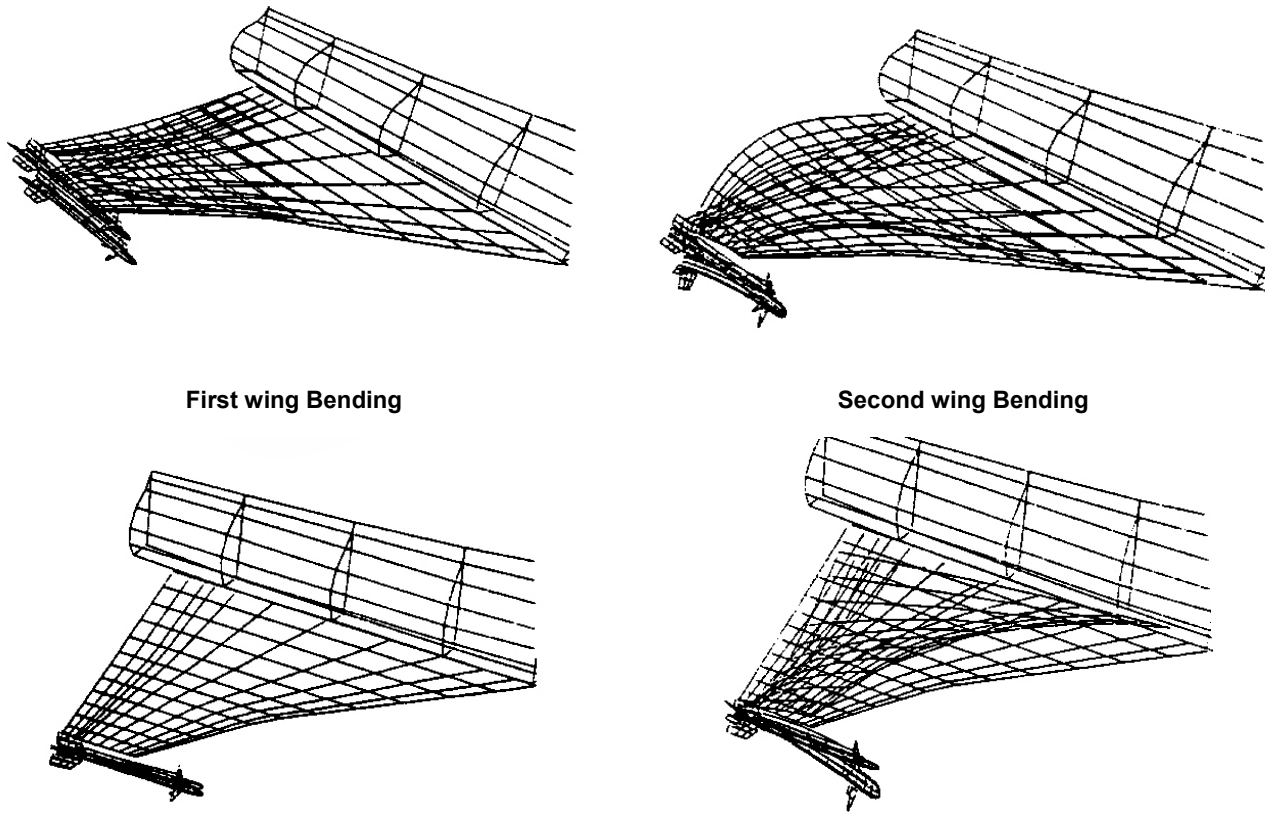

First wing Bending

Second wing Bending

Missile pitch

First wing Torsion

Figure 3: Vibration Modes.

Figure 4 documents very high accelerations on the tip mounted missile due to discrete gust caused mainly at short gust length (18 m) by the second elastic mode of the wing and also shows alleviation effect of the elastic wing on the response at long gust length (144 m) compared to the rigid response (full line).

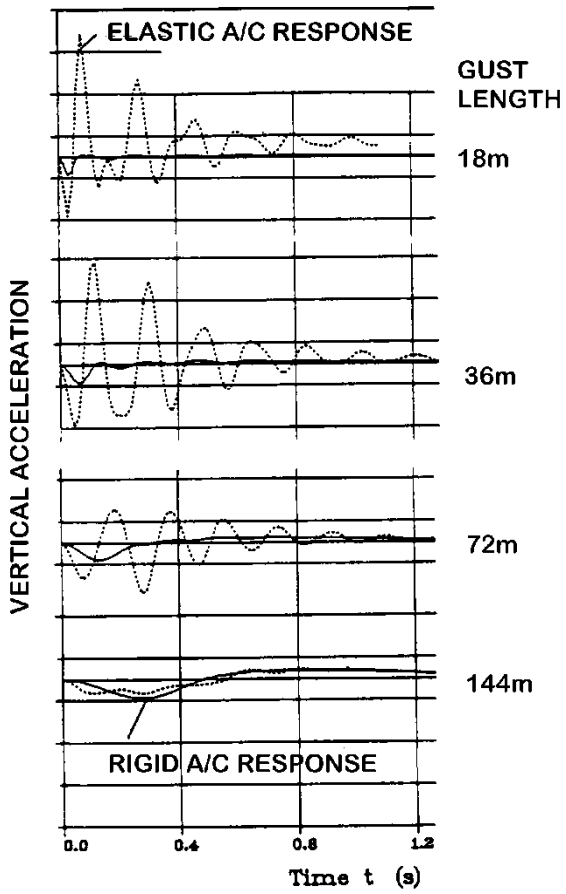

Figure 4: Discrete Gust Analysis – Acceleration at Missile Nose.

3.0 EFFECT OF BUFFET ON AIRCRAFT STRUCTURE, EXTERNAL STORES, EQUIPMENT AND RIDE COMFORT

The structural design of wing, fin, rear and front fuselage, external stores, airbrakes and engine attachments is affected by buffet, Figure 5. Besides the structural design of main aircraft components also the equipment, the equipment trays and equipment qualification is influenced by buffet and the vibration levels at the pilot seats are affected.

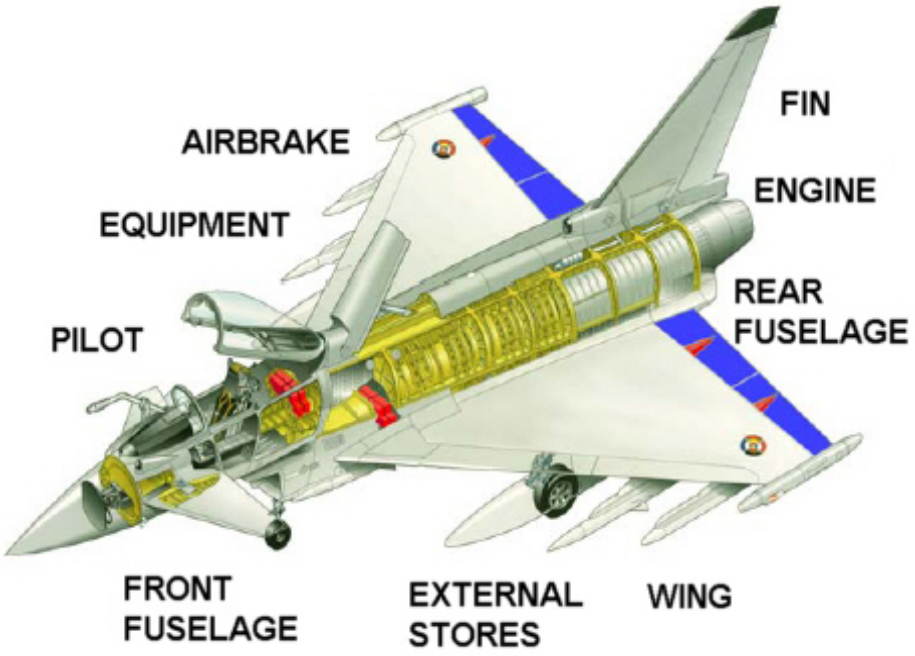

Figure 5: Aircraft components affected by buffet.

Generally speaking the structural design in view of buffet can be distinguished into:

1) Structural Design
   Predicted dynamic buffet loads for the design of the following components:
   - Fin structural design (not covered by tuned gust analysis.
   - Rear/center fuselage structural design.
   - Wing buffet (covered by tuned gust analysis).

2) Equipment design and qualification
   Predicted and flight measured buffeting vibrations are applied for the vibration qualification of equipment in front/center/rear fuselage and avionic bay and external stores on wing and fuselage.

3) External Stores qualification
   Predicted and flight measured buffet vibrations are applied for vibration qualification of stores and missiles underwing and on fuselage.

4) Pilot discomfort
   Predicted buffeting vibrations are used to assess the pilot comfort.

3.1 Buffeting Prediction Procedure

Methods are well established for the calculation of the flexible aircraft in turbulence and in buffet conditions, see Refs. 1 to 4. In general it is the solution of linearized flight dynamic equations of motion of the aircraft with coupled structural dynamic equations in frequency and in time domain. The dynamic response approach using linearized equations of motion of the aircraft around trimmed condition coupled with structural dynamic equations and flight control equations will give the possibility to introduce the unsteady and coupling effects in a proper sense. Therefore flight dynamic and structural dynamic responses are described in the right phase and the superposition of vibration and dynamic loads from both contributions can be

performed. With the linearalized model the transfer functions of all state variables, of local accelerations and of dynamic loads due to a buffet excitation input can be calculated

The procedure for the determination of buffeting is outlined in Figure 6. The buffet excitation is derived from buffet wind tunnel models. The dynamic response, i.e. the buffeting of the aircraft is determined through total aircraft response calculations leading to local vibrations and local dynamic loads. Modal analysis applied for dynamic response calculations on the basis of a finite element model of the aircraft; unsteady aerodynamic forces of the flexible aircraft modes are calculated using lifting surface theory.

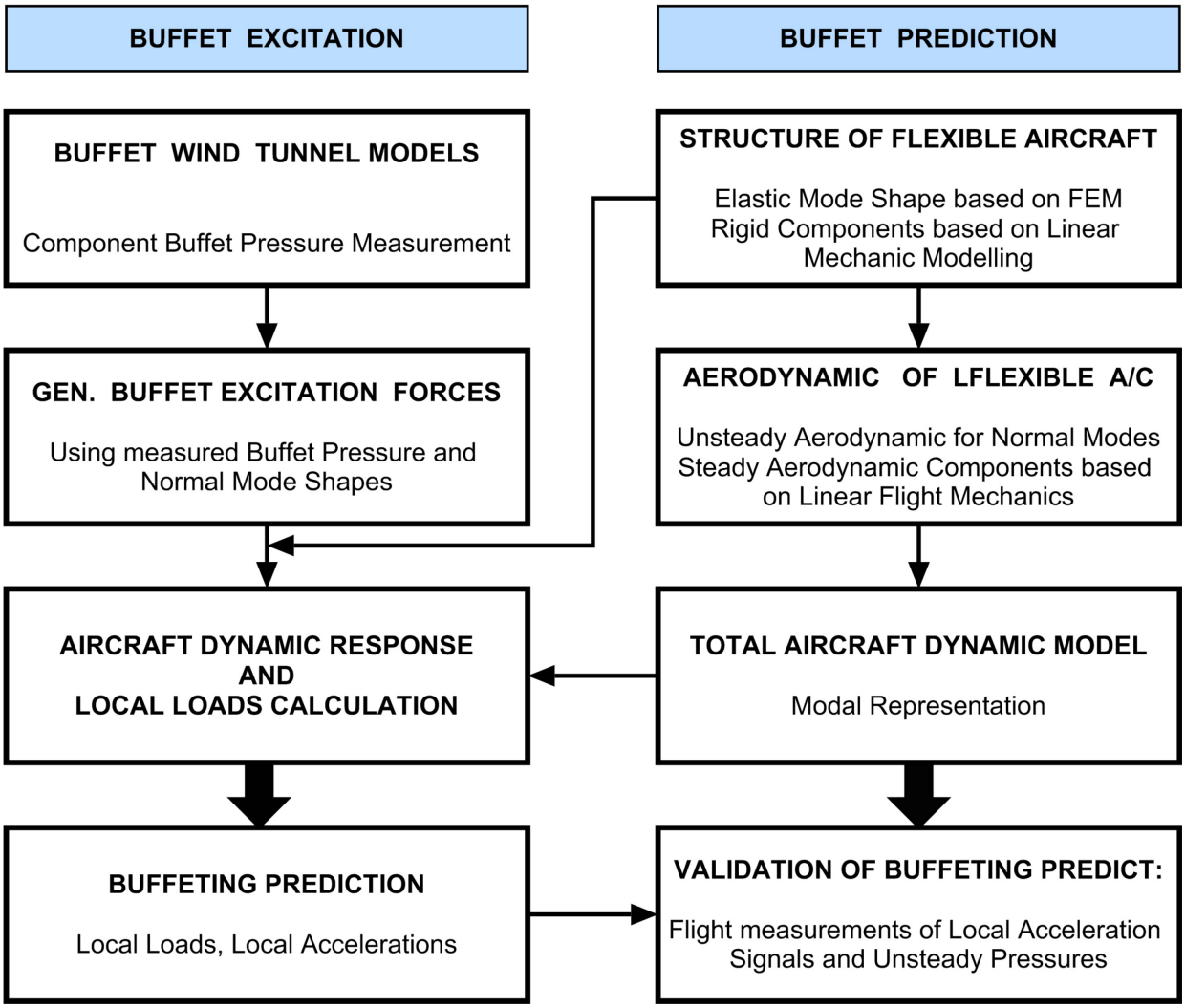

Figure 6: Procedure for the buffeting prediction.

In summary the following assumptions can be drawn for the applied prediction method:

- Buffet forces are not influenced by harmonic aircraft elastic modes and therefore can be measured on “rigid aircraft” wind tunnel model.
- Buffeting response, local accelerations and local dynamic loads can be derived by using an analytical model (FEM) for dynamic response calculations.
- Validation of the above assumptions was performed during TORNADO development program on windtunnel tests as well as on flight tests.

3.2 Results from Windtunnel Tests

Strong non-linear effects caused by leading edge vortex flow are apparent at the main parts of the wing with the indication of inner wing area reattached flow up to incidences of about α = 8 deg. depending on Mach number or dynamic pressure and outer wing trailing edge flow reattachment up to α = 6 deg. Wing tip flow separation effects are observed starting at 6 to 8 degrees, the negative pressure at the outer wing section decreases then with increase of incidence. The inner wing pressure distributions are strongly affected by the interaction with the canard, whereas the flow and flow separation at the wing tip region is hardly affected by the static canard deflection.

3.3 Fluctuating Pressures

Fluctuating pressures at constant static incidence are of interest for the prediction of the structural dynamic response for the buffeting prediction. The power spectral density of exciting forces and its dependency of the static incidence and of Mach number in Figure 7 demonstrates time histories of two pressure signals at M = 0.8 and 10 degrees, with peak values cp = *0.12*.

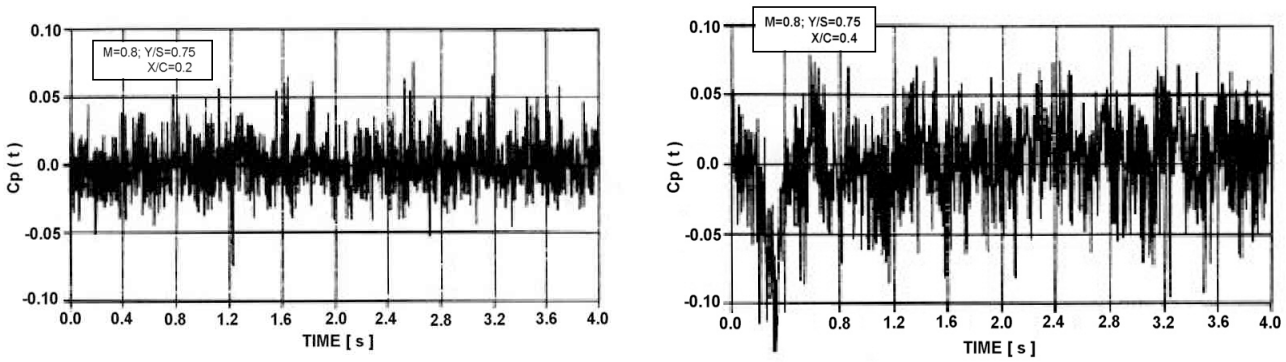

Mach=0.8; Y/S=0.75; X/C=0.2 **Mach=0.8; Y/S=0.75; X/C=0.4**

Figure 7: Wing buffet – Time history of a wing buffet pressure.

3.4 The Major Features of the Buffet Excitation Forces are:

- Broadband characteristic of the PSD in the frequency region 0 - 100 Hz with no decay at incidences 6, 8 and 14 deg. and no specific peaks at the frequency of the first bending at 35 Hz.
- Strong increase in the amplitude from 6 to 8 degrees of static incidence followed by smaller increase with incidence.
- Effect of Mach number on the PSD is small, the modulus of the PSD is similar for Ma = 0.3 and Ma = 0.6 and is less to some small amount at Ma = 0.9.
- The coherence formulated for pairs of pressure signals is in general very small. The coherence of neighboring signals is highest but the value is always less than 0.4 indicating only very small correlation of fluctuating pressures.

3.5 Comparison of Measured and Predicted Dynamic Response of Windtunnel Model

The buffeting prediction method has been validated by comparisons of predicted and measured dynamic responses on the TKF wing model, see Figure 8 and 9, which show good correlation in the power spectral densities for different locations and flexible modes.

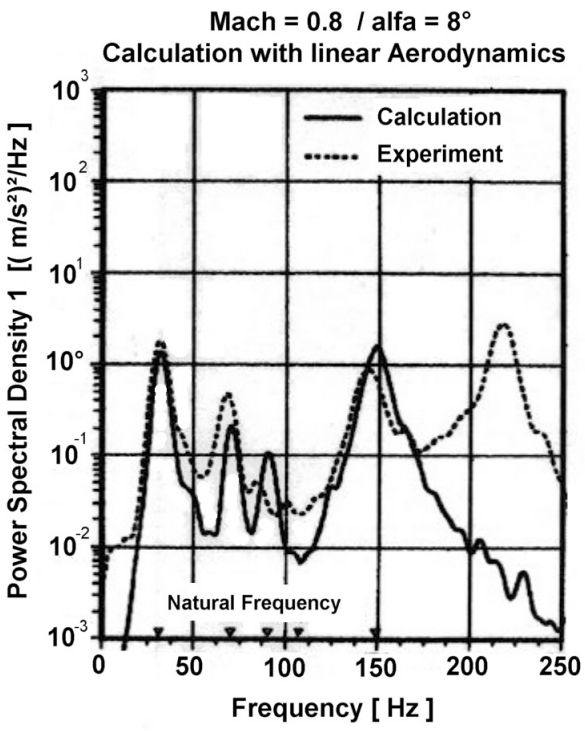

Figure 8-1: Validation of buffeting prediction method – Comparison of predicted and measured wing model responses, Mode 1.

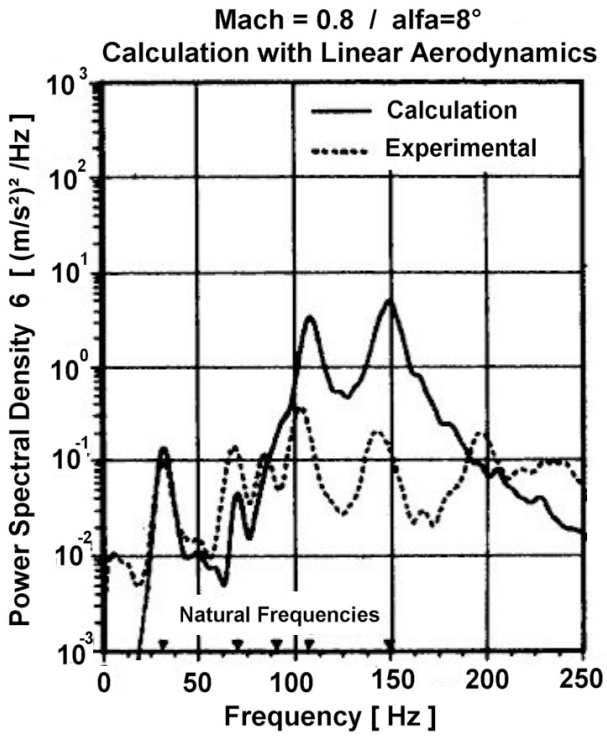

Figure 8-2: Validation of buffeting prediction method – Comparison of predicted and measured wing model responses, Mode 6.

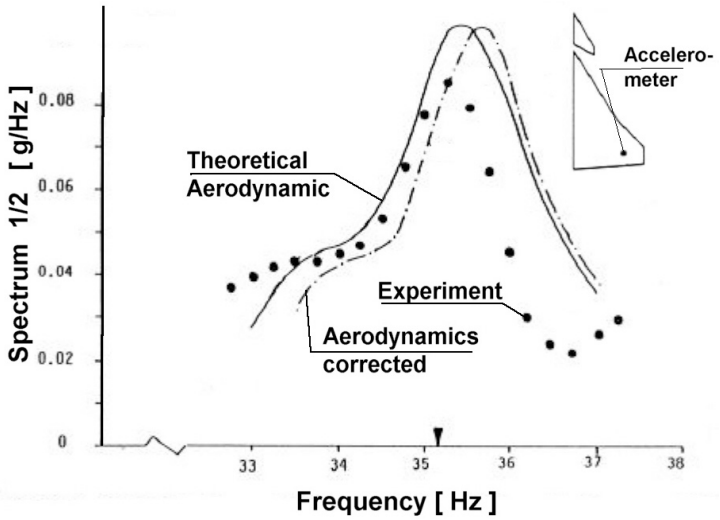

Figure 9: Wing buffet prediction – Comparison of predicted and measured model responses.

3.6 Comparison of Prediction to Flight Test Results

The buffeting prediction was validated for the aircraft substructures by in flight measured vibrations and wind tunnel tests. Figure 10 demonstrate comparisons of wing tip acceleration response trends versus incidence for Mach=0.75 and altitude between 265000 and 38400 ft. A reasonable good correlation between prediction and test was found which again confirmed the validity of the wing buffeting prediction

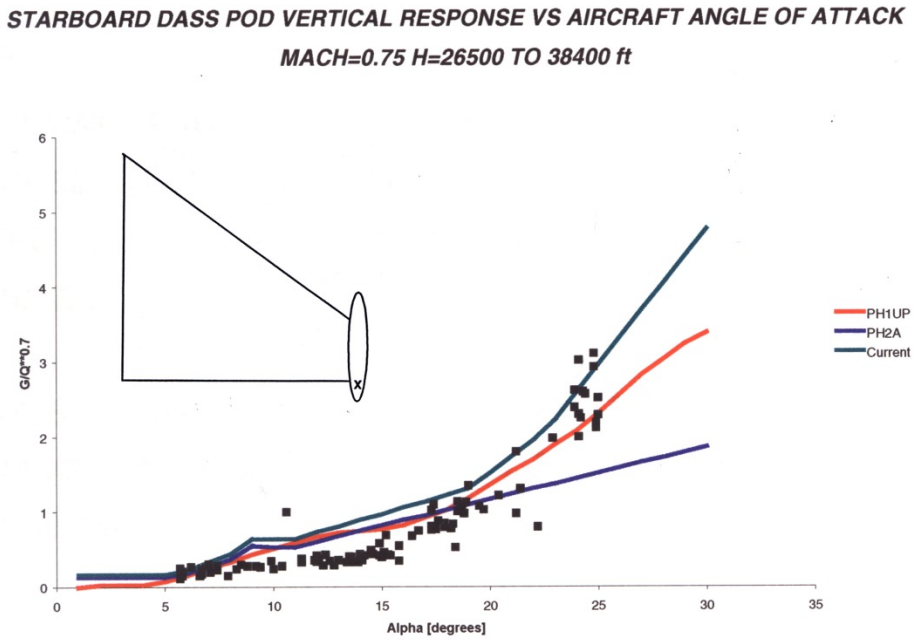

Figure 10: Wing Tip Pod buffeting prediction – Comparison of predicted and flight measured wing response trends with incidence on rear wing pod vertical.

Figure 11 depict comparisons of underwing AIM9L Missile horizontal acceleration response trends versus incidence for different Mach and altitudes and Figure 12 shows the underwing AIM9L Missile vertical acceleration also for different Mach Numbers and Altitudes. A reasonable good correlation between prediction and test was found which again confirmed the validity of the wing buffeting prediction.

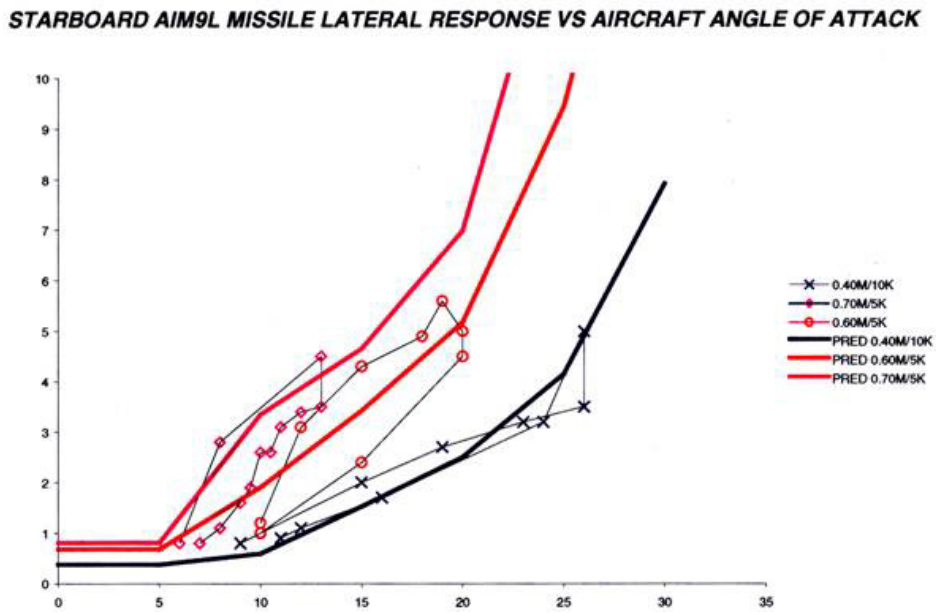

Figure 11: Store buffeting prediction – Comparison of predicted and flight measured wing response trends with incidence, for Starboard AIM9L Missile Lateral.

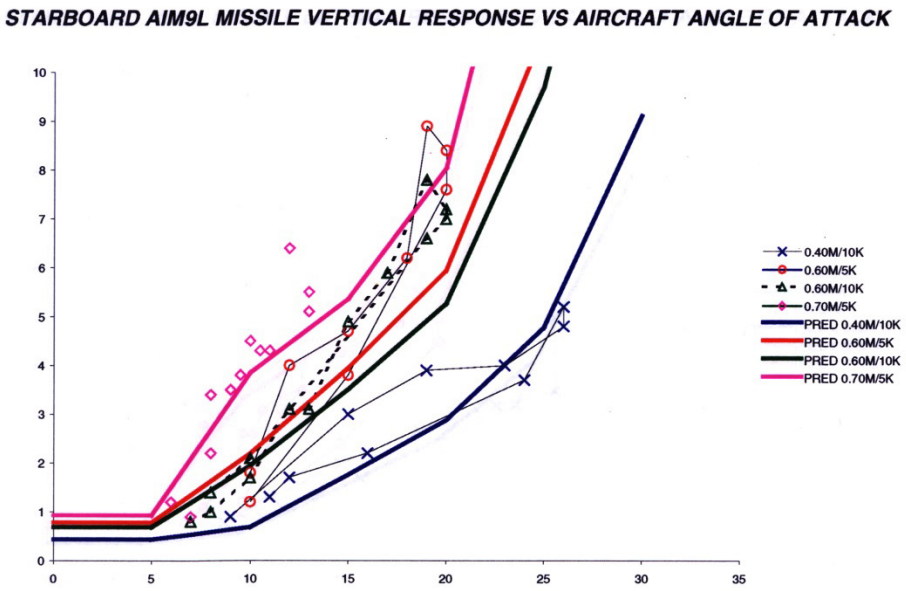

Figure 12: Store buffeting prediction – Comparison of predicted and flight measured wing response trends with incidence, for Starboard AIM9L Missile Vertical.

With these diagrams it should be pointed out, that due to buffet excitation the dynamic response on the external underwing and under fuselage stores are reasonable and have to be considered in Design of Stores and during the clearance phase.

Figure 13 demonstrates the buffeting prediction of center fuselage. The comparison of tested and predicted PSD at a defined center fuselage location shows lower test values for a high number of flight conditions. The result is applied for verification of equipment and under fuselage store vibration qualification.

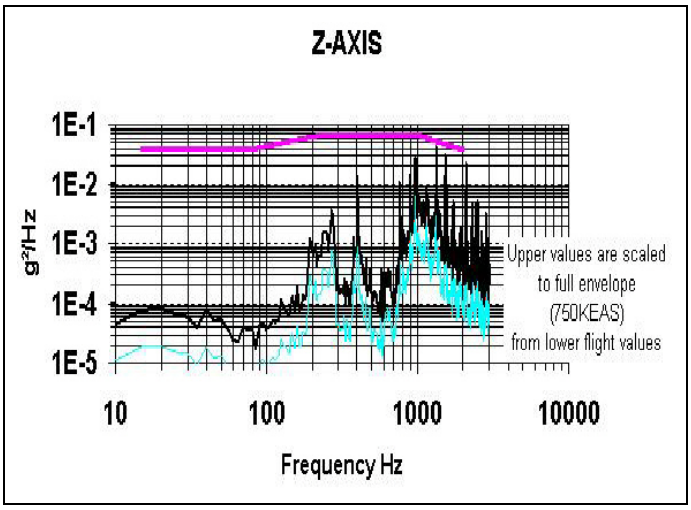

Figure 13: Center fuselage buffeting prediction – Comparison of tested and predicted PSD for equipment qualification.

4.0 LANDING IMPACT

Modern combat aircraft are designed for multi role military missions, performing air superiority, reconnaissance and ground attack. Therefore a large number of different external stores must be integrated during development and production phase of the aircraft. During the landing impact, the external stores generate high dynamic loads on the undercarriage, the landing gear attachment points and on the aircraft structure. During taxi of the aircraft with underwing stores in some cases the ground loads are very high due to roughness on the runway and high taxi speeds.

A method has been developed for prediction of the dynamic loads, taking into account ground and flight test results. The computations are based on a general dynamic model including a non-linear model of the landing gear and the tire. The aircraft model can be used with and without external stores. In the first step dynamic loads are generated due to the landing impact on the main wheels and used as design and clearance loads of the undercarriage. In the second step the attachment loads of the undercarriage are used as input for the excitation of the aircraft structure. Symmetric landing impacts as well as crosswind landings with different sink rate and external store carriage have been investigated and will be discussed in the paper.

Loads of all different ground maneuvers have been analyses. Besides the normal landing in a symmetric carriage configuration, also heavy asymmetric external store carriage has been investigated. Rejected take off loads, arrested landings loads, towing, turning and symmetric and asymmetric braking loads have been analyzed for hot, normal and cold days. Results from loads analysis on repaired runway with minimum single spacing mats of 130 m will be shown and the difference on loads during wet and try runway landing impacts.

The different phases of the landing impact forces are shown in principle in Figure 14. In normal approaches it starts with the main gear impact, after the derotation with the nose gear impact and on both gear during breaking. In particular the chute landing impact, the arrester hook landing impact and the rough runway impact must be investigated.

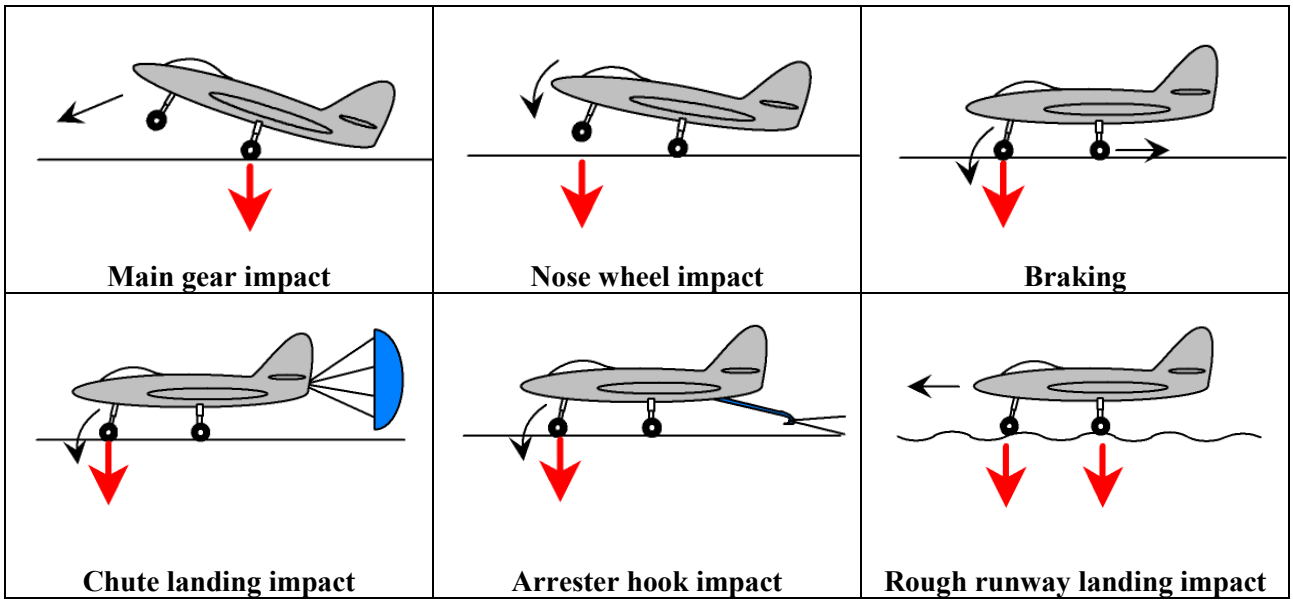

Figure 14: Different phase of landing impacts.

4.1 Main Analytical Results

The model description allows to predict, early in a development program or in the clearance procedure, the level of loads acting on the landing gear, the aircraft structure and the external stores during landing impact phases.

The landing gear model combined with the aircraft model enables to analyse the influence of physical parameters on the dynamic response of the aircraft carrying external stores and provide load envelopes for clearances or specifications for design.

Main results which can predict are the dynamic coupling between the landing gear and the elastic aircraft structure and between external store elastic modes with aircraft elastic modes. In case of new external store development the store can be modified early in the program to avoid restrictions in the flight envelope and damaging coupling of the system.

On the aircraft side different parameters act on the frequency of elastic modes and therefore influence the dynamic response behaviour of the vehicle. For instants the amount of fuel can change the fuselage modes and the different weight of the external stores can also change the dynamic characteristic of the elastic aircraft. For a new store development and the landing gear itself a robust load specification must be delivered.

During the development of an aircraft a lot of configurations must be considered to design the aircraft structure and the landing gears. To shorten this work a couple of mass key configurations were chosen. In principal the heavy weight of an aircraft influences the design of the landing gear due to the high loads during impact. The shock absorber as well as the landing gear must be tuned together to withstand the high peaks of the landing impact. In practice, the sink rates for aircraft are lower in heavier weight configuration. The aircraft structure itself has a vice versa behaviour. Due to the heavy masses on external pylons the aircraft structure shows lower excitation during the landing impact.

Figure 15 depicts in a three side view the loads on the star port gear during an asymmetric impact. In this case the star port gear touches the ground first. The blue curves show the loads for the three axis of the centre wheel, the red curve is the summary of the three blue curves, which shows the resulting loads after the impact. Figure 16 shows the loads after the aircraft for the port gear with the same explanation of Figure 15. It is worth to mention, that the loads are higher on the port gear, which is the second impact a as on the star port gear which is the first impact on an asymmetric landing. These loads will be transformed to the attachment point of the landing gear. The elastic gear as well as the nonlinear shock absorber will be taken into account at the transformation procedure. This attachment forces or loads will be used as an inner excitation of the aircraft structure itself. Figure 17 shows the complete landing in the time domain for port and star port wheels for the main landing gear. The important phases are marked, as spin up and spring back movement and the inboard and outboard movement of the star port and port landing gear.

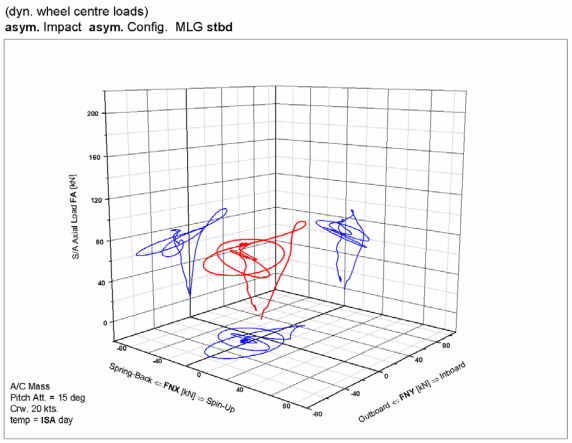

Figure 15: Three side view of dynamic wheel centre loads of star port main landing gear at asymmetric impact.

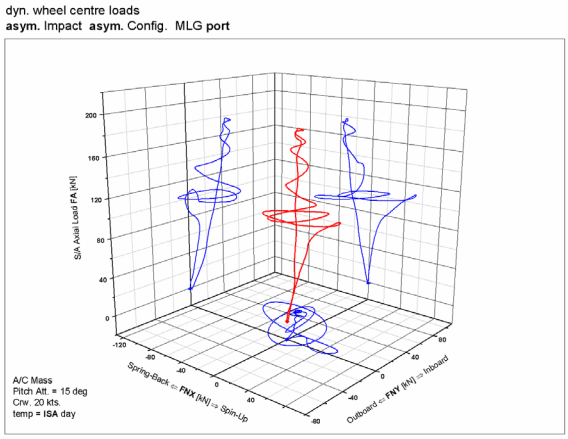

Figure 16: Three side view of dynamic wheel centre loads of port main landing gear at asymmetric impact.

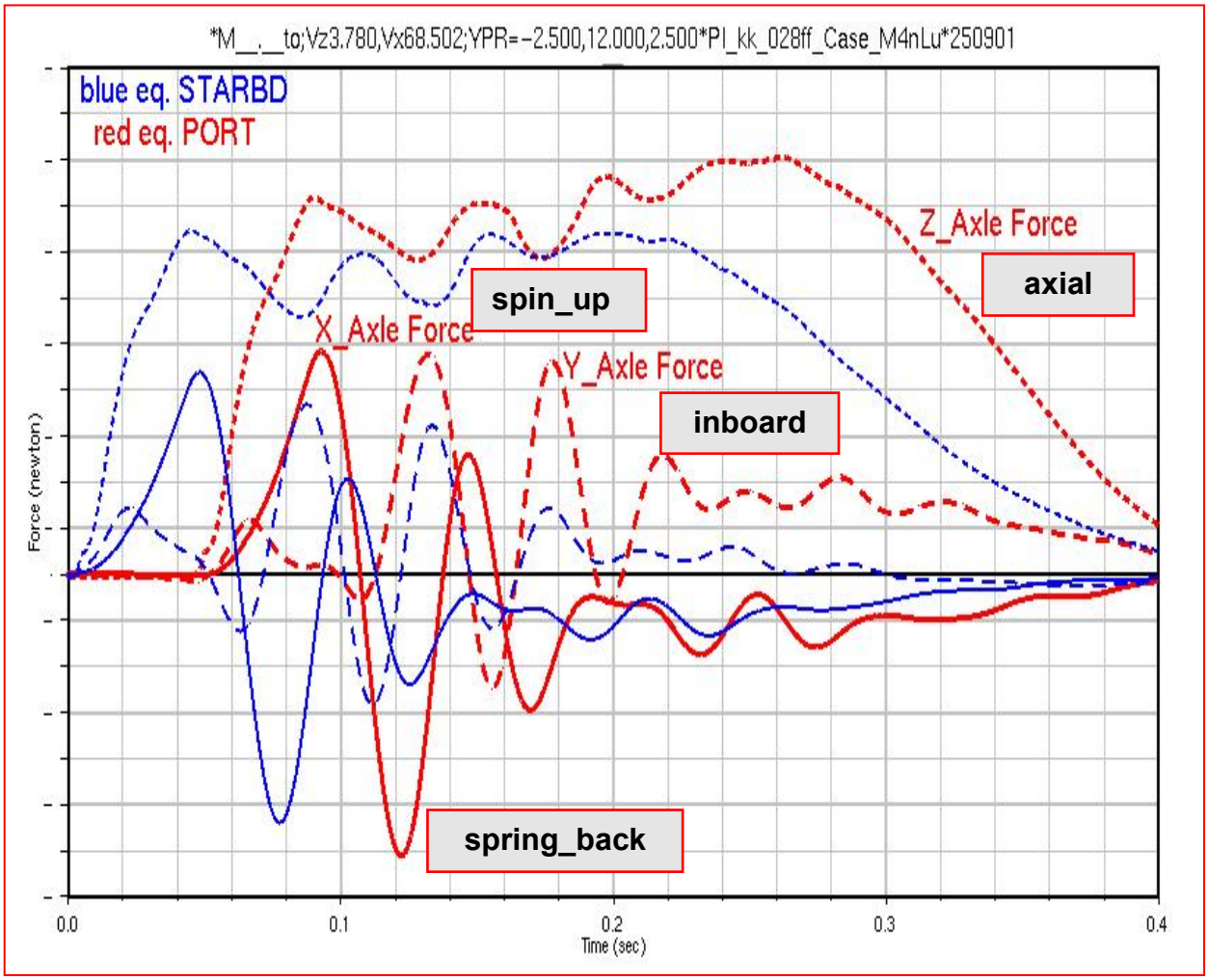

Figure 17: Time history of port and star port main landing gear at asymmetric landing impact.

Figure 18 compares the vertical acceleration of the right forward wind tip pod. The black line shows the test results and the green line the calculation. This figure demonstrates that the dynamic system is well described because the frequency and the magnitude of the dynamic response are well predicted. This data is used to update the dynamic system and to predict in case of store integration the dynamic loads for the specifications.

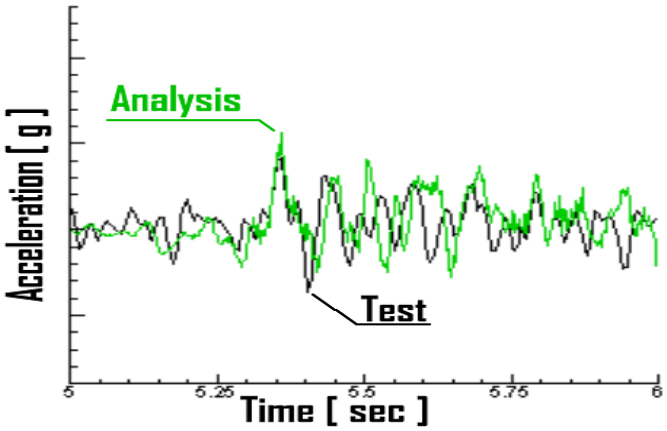

Figure 18: Comparison of test and analysis for forward wing tip z-acceleration.

Using the flight test results to update the dynamic model and transform the ground or axle loads from main landing gear wheel to the attachment points of the gear. With this input a dynamic response analysis will be performed. Figure 19 shows the result of a store integration analysis. The calculated loads (red area) are compared with the allowable load envelopes (Ale's – green area). This example discusses the loads on the interface of a pylon with a heavy store mounted. As it can be seen in Figure 21 the Mx versus My exceeds the allowable load envelope. In this particular case the sink rate for this external store configuration must be restricted or the store must be tuned to keep the loads inside the allowable loads envelope.

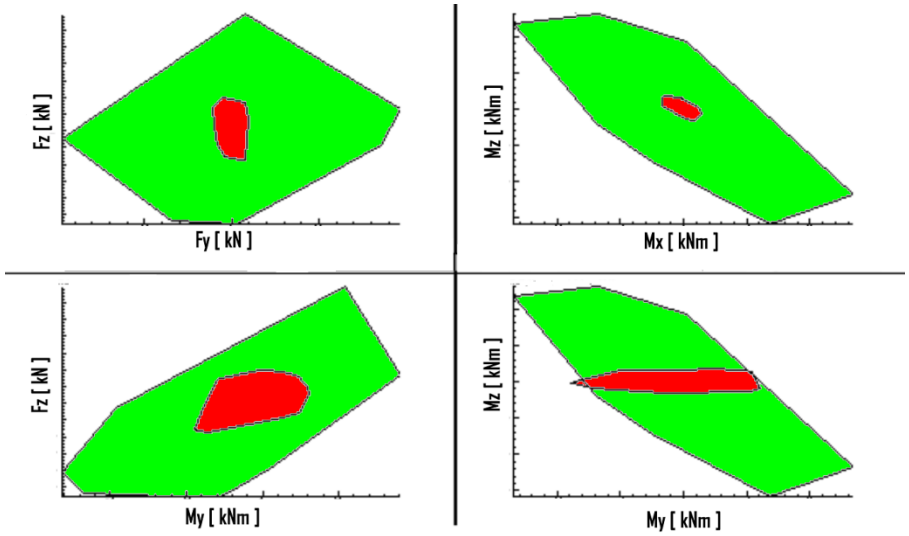

Figure 19: Load Envelopes at pylon interface.

Figure 20 shows the Load envelope for the main landing gear attachment for the pintle Lz versus Lx. All investigated landing impacts are shown with different marks. It turned out, that the critical maneuver for this

aircraft is the min. mass configuration, because there is no restriction for the sink rate values. In this analysis the max. sink rate was assumed.

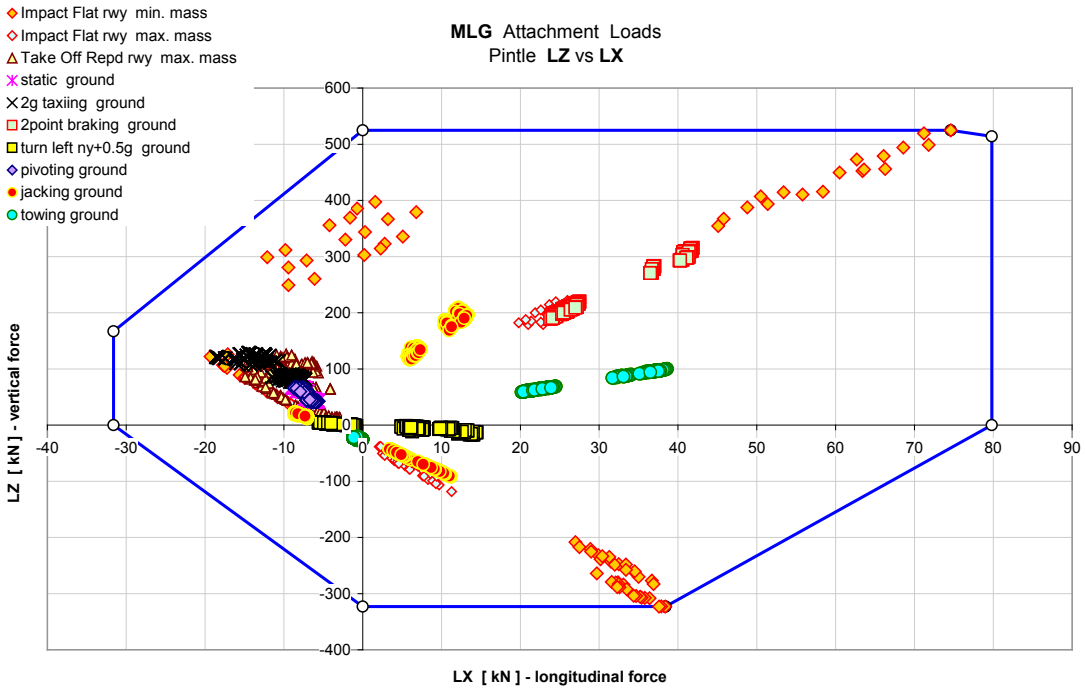

Figure 20: Load Envelopes for Main Gear attachment.

4.2 Conclusion – Landing Impact

This methodology enables to integrate and to certify on each external aircraft pylon stations very different types of stores in terms of weight, stiffness and centre of gravity and in the early development of new weapons to create a very robust store specification in terms of dynamic response.

In case of store development the process have to start at the very beginning of the store development in order to provide for the Design department reliable specifications.

In case of certification of the store, the data can be used to reduce ground testing due to precise predictions. Therefore the integration of a new external store can be done in a minimum of time and cost.

5.0 STORE POINTING ERROR DUE TO FLEXIBLE AIRCRAFT

5.1 Principles of Alignment

The aircraft system design and performance specification requires providing alignment accuracy's of specific sensors navigational support or weapon devices in order to minimize errors in navigation, maximize weapon delivery accuracy and optimize flight control response. "Harmonization" describes the alignment of all sensors, displays and weapons to a fixed and common airframe datum. Important candidates are the avionics system which comprises head up display, laser inertial navigator, radar, forward looking infra-red system, armament stations etc. and flight control system candidates like inertial measurement unit and air data transducers. The alignment reference point for both the avionics and flight control system is traditionally chosen as a fixed longitudinal fuselage airframe Datum, common in application to both ground alignment

checks and mathematical modeling analysis of in-flight airframe behavior. The position of the fixed reference line coincides in position with the aircraft body axis coordinate system. Devices installed with their longitudinal datum at fixed offsets to aircraft Longitudinal Fuselage Datum (LFD), will be subject to datum translation through the offset angles. Physical representation of LFD is achieved by establishing hard point references in the nose wheel bay of the aircraft which is identified as the most stable part.

The setting up of these references is accomplished as part of the overall symmetry and alignment procedure, carried out during aircraft manufacturing. The points of symmetry themselves are confirmed during marry up of the main airframe components. The symmetry and alignment test procedure establishes angular positioning of the attachment tool to an accuracy of 0.1 mrad in pitch, roll and yaw.

5.2 Error Sources

Two major groups of error sources for misalignment are identified:

- Ground Static Error.
- Flight Static Error.

The first group of errors is installation attributable due to aircraft build, mounting tray manufacturing tolerances and harmonization tooling errors. Three sources of ground static alignment errors are considered to result from the basic build of airframe:

- JIG tolerances: The main airframe sections incorporating installation points for harmonization candidates are assembled in separate Jigs under conditions which are considered to be similar to zero ‘g’ conditions.
- Airframe Marry up Tolerances: “marrying up” considers the final assembly of the airframe which incorporates symmetry and alignment checks for verification on the completed assembly.
- Airframe settling: After first flight of the aircraft, the airframe shall be subjected to a settling process which will result in further alignment error contribution.

Ground Static Errors confirmation will be determined by actual measurement in relation to the aircraft reference datum, using on ground tooling. Such errors are corrected on the basis measurement data, applied via software methods implemented in flight or as mechanical adjustment.

The second group comprises Flight Static Errors. Changes in the alignment of each candidate objective to Harmonization will vary according the candidates structural characteristics according the location within the airframe and the elastic deformation characteristics of the airframe. Aircraft structure elastic behavior is caused by flight maneuvers inducing aero-elastic deformations. Strictly speaking with respect to a preliminary assessment of candidate misalignments, their magnitudes, characteristics and compensation, the harmonization process focuses its attention to non-transient combat flight maneuver phases.

5.3 Harmonization Scheme and In Flight Data Transfer

Airframe elastic deformation is dependent predominantly in aircraft LOAD configuration e.g. external store configuration and fuel mass distribution, dynamic pressure, Mach-number and aerodynamic trim variables for longitudinal and lateral flight case with restrictions to steady state maneuvers. Assessment of Flight Static Errors is carried out using Finite Element Method techniques for airframe as well as for aerodynamic modeling. The alignment error compensation bases finally on sophisticated software methods using stored correction data in the form of Look up tables and applied processing algorithm, co-resident in the non-volatile memory of each candidate.

For aircraft throughout the flight the following transfer takes place: Specific aircraft parameters e.g. Load-category, angle of attack and Mach number is mentioned by an onboard central computer and then

categorized into integer form. This information is transmitted to the candidate equipment processor and is used as an address indicator for locating valid Look up table (LUT) data. For given candidates the data is contained in Look up table blocks, each block is representative of a specific aircraft store and mass configuration. Each table block is further arranged in a multi spreadsheet form, as a function of angle of attack and Mach-number, possessing cell information for displacement derivatives. The LUT-data is extracted at a high rate and made available for use in a predefined linear translation algorithm for determination of overall angular Flight Static correction terms in pitch, roll and yaw including Ground and Flight static correction.

5.4 Analyses Method – Structure Deformation Behavior

5.4.1 Finite Element Model of the Structure

The aircraft was dynamically modeled by a 6 degree of freedom finite element model which fully represents the total aircraft stiffness and mass.

The clean aircraft was split up into different substructures, namely, foreplane, wing with flaps and slats, fuselage, fin and rudder. All substructures stiffness matrices were calculated with MSC NASTRAN, starting with a very fine static finite element model Figure 21, applying a dynamic condensation to a coarse dynamic model. For the fuselage generalized and equipment points were generated. Port and starport of the structure is assumed to be symmetric which allows to create only a half model with symmetric and antisymmetric boundary conditions applied to the symmetry plane.

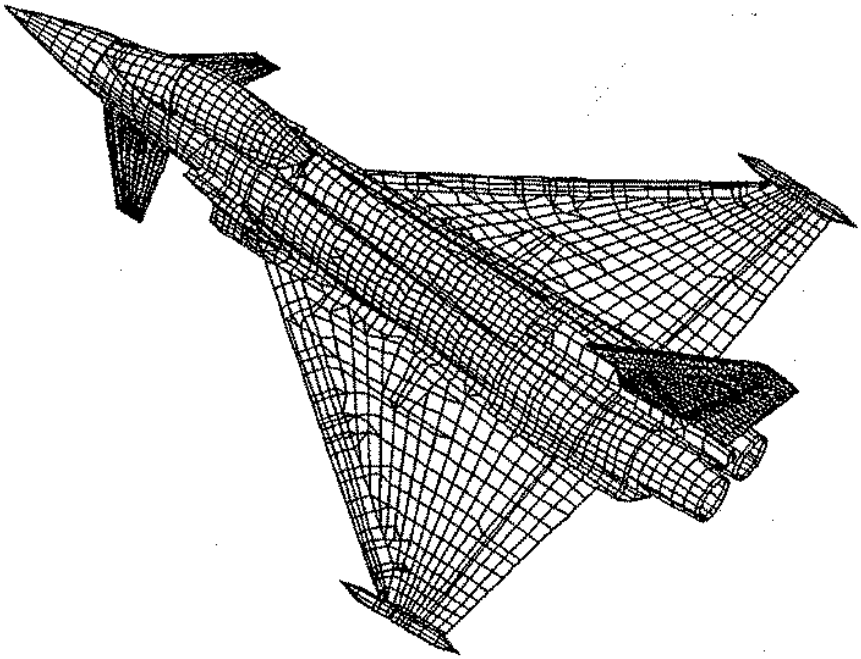

Figure 21: Finite Element Model Aircraft, static fine mesh.

Some details of the model:

- The dynamic FE-model used for Modal approach represents only a half model and cannot describe antisymmetric store configurations. For Harmonization purposes assumptions are made to cover symmetric and asymmetric store configurations. Structural coupling between port and starport wing hardpoint locations are of minor influence due to the almost rigid stiffness behavior of the center

fuselage. However, for each wing locations, port and starport, individual calculations are performed with corresponding symmetric store configuration.

- Pylon flexible structure is included in FEM via NASTRAN GENEL elements.
- Nonlinear structural behavior due to backlash effects at connection parts on pylon, wing, missile are not modeled and not considered with any reduced stiffness values.
- Missile structure is assumed to be rigid.
- Fuel status for wing internal and external tank as well as fuselage tank are model by concentrated masses.

5.4.2 Aerodynamic Model

Aerodynamic loads are calculated with linear potential aerodynamic in-house codes applicable for subsonic and supersonic flight conditions:

- Steady and unsteady aerodynamic forces are calculated at four Mach-numbers (0.7, 0.9, 1.2, 1.6).
- Stores are not modeled as aerodynamic bodies.
- Lifting surfaces are assumed to be plain surfaces in the aerodynamic model neglecting camber or twisted shape of aircraft wing. Hence zero lift wing deformation will be considered in Harmonization process as an additional term in wing deformation algorithm.
- Ranges of incidences are defined, nonlinear behavior of lift forces are taken in consideration as additional correcting factors for sensitivities in the deformation algorithm.

5.4.3 Modal Analysis Approach

The Modal formulation of system equations is fundamental to Modal Analysis Approach of elastic structure at dynamic analysis. As a first step eigenvectors are calculated using basic NASTRAN solution. In the second step the eigenvectors are used to reduce the originally given modal degree of freedoms into a smaller set of generalized coordinates:

$$[K_{aa} - q * Q_{aa}] * [u_{aa}] = q * [Q_{ax}] * [u_x] + [P_a]$$

where:

$[Q_{aa}]$	generalized aerodynamic forces
$[Q_{ax}]$	generalized aerodynamic forces due to surface deflection
$[K_{aa}]$	generalized stiffness
$[P_a]$	generalized applied loads (= external loads)
q	reference dynamic pressure

Sensitivities are derived from the above equation, using unit cases of relevant aerodynamic flight parameters like angle of attack, flap deflection. Aerodynamic effects show a variation with e.g. fuel quantity, these sensitivities are not purely unit cases of the relevant parameters. Due to modal analysis approach, inertia effects will be also represented by these sensitivities. As an important consequence of this, some sensitivity depending on inertia parameters can be ignoring the overall deflection algorithm. Only stationary maneuvers can be simulated by the used modal approach and therefore deflections induced by unsteady motions are neglected. Acceleration forces due to rigid body motions having nonlinear characteristics are outside of modal approach capabilities.

5.5 Correction of Sensitivity Terms

5.5.1 Effect of Influence on Deformation Sensitivities

The sensitivities used for harmonization algorithm is based on pure linear theoretical aerodynamic forces. In order to introduce the nonlinear relation between incidence and lift force into the harmonization algorithm the aerodynamic dataset of the demonstrator A/C will be corrected.

Four ranges of incidence are defined:

- Range 1: $-15.0° < \alpha < -5.0°$
- Range 2: $-5.0° < \alpha < 10.0°$
- Range 3: $10.0° < \alpha < 25.0°$
- Range 4: $25.0° < \alpha < 40.0°$

For the above reasons the delta linearization of the specific aerodynamic function is applied, in view of minimizing the introduced error into the correction procedure and to simplify the handling of the harmonization procedure.

Figure 22 and 23 shows as an example the correction terms for the $alfa_0$. This must be introduced into the harmonization process, because this correction is not introduced into the theoretical aerodynamic data functions and it is essential for the sensitivities in the look up tables. In principal, the correction terms are decreasing up to Mach No = 1.0 and after the sound barrier increasing.

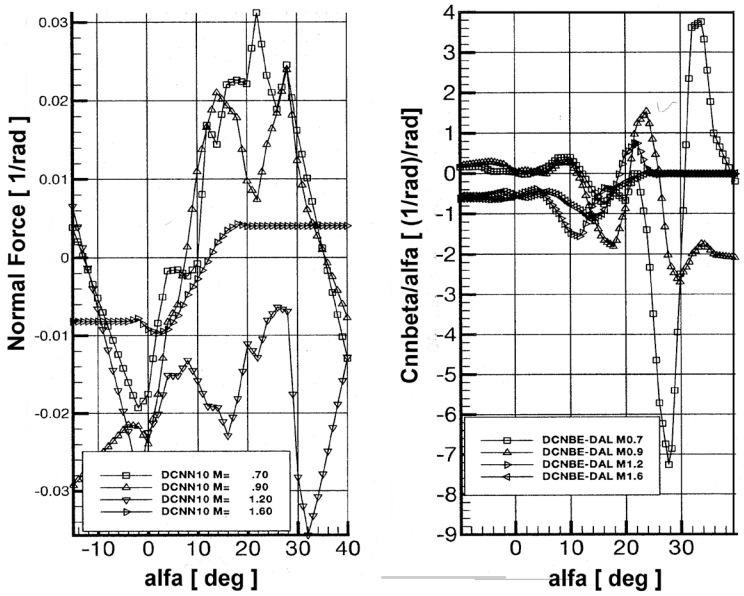

Figure 22: Aerodynamic Functions, normal lift force, yaw-moment.

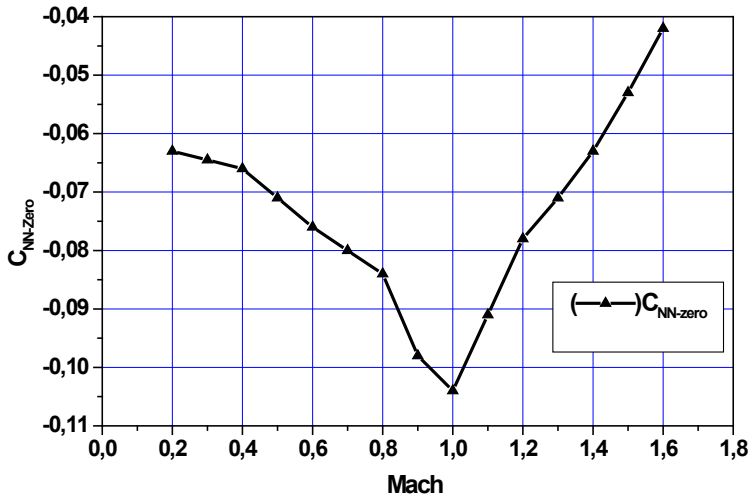

Figure 23: Zero Incidence Lift Coefficient versus Mach number.

Figures 24 to 27 show the correction factors for different aerodynamic forces or moments. Due to the large variation of the correction factor is assumed that inside the chosen interval of angle of attack (AoA) the numbers can be taken as a mean value.

Figure 25 shows the so called mean numbers of the correction factor of the theoretical aerodynamic dataset (Figure 24) for the normal lift force on the trailing edge. Figure 27 shows the mean numbers of the correction factors of the theoretical aerodynamic dataset (Figure 26) for the roll damping.

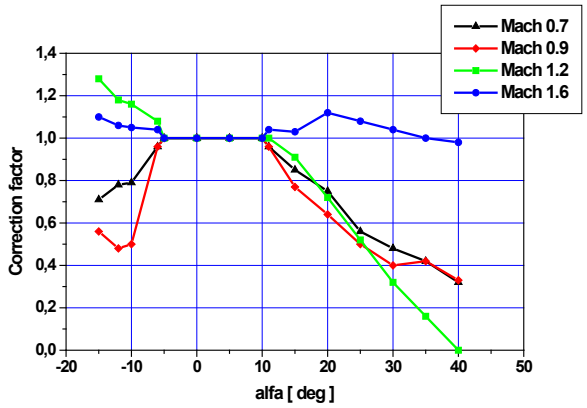

Figure 24: Normal Force trailing edge flap correction factor to theoretical aerodynamic dataset.

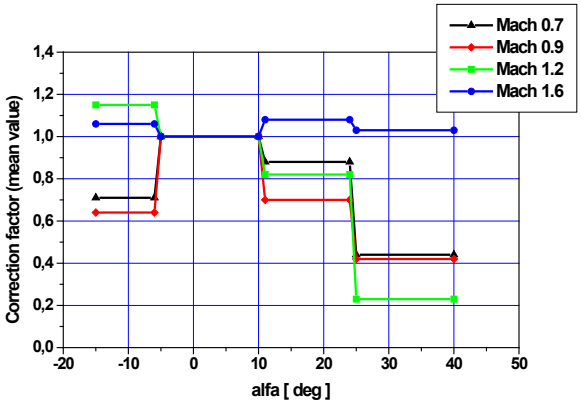

Figure 25: Normal force trailing edge flap correction factor (mean values) for theoretical aerodynamic dataset.

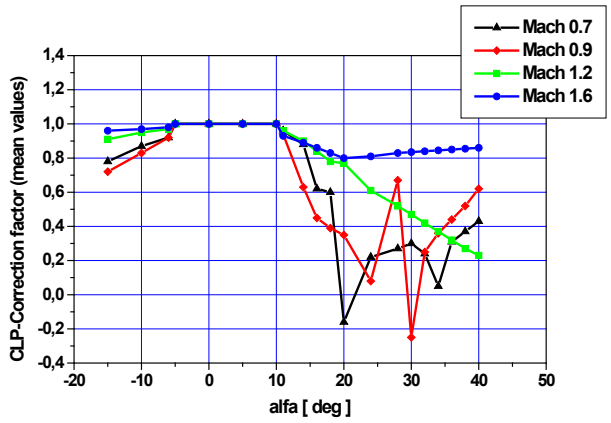

Figure 26: Roll damping correction factor for theoretical aerodynamic dataset.

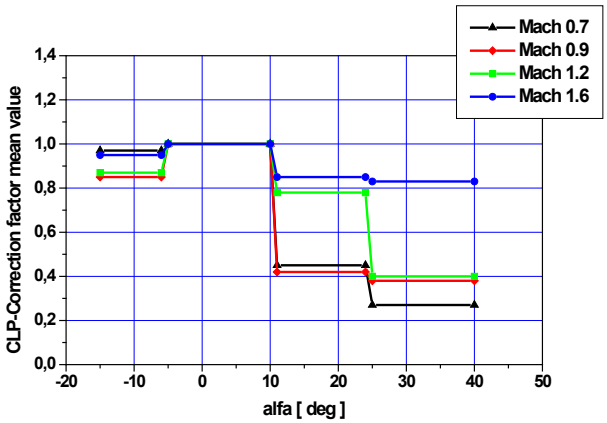

Figure 27: Roll damping correction factor (mean values) for theoretical aerodynamic dataset.

Table 2 summarizes as an example all applied correction factors for the four investigated theoretical aerodynamic Mach numbers. The range R2 is set to 1.0, because this is the range where the aircraft normal flies and this is therefore the basis for all theoretical aerodynamic databases.

Table 2: Summary of correction factors.

Factor		M=0.7	M=0.9	M=1.2	M=1.6	Sensitivity
Normal Force DC_{NN}	R1	0.914	0.859	0.933	0.995	Pitch due to AOA Pitch due to F/P deflection Roll due to AOA
	R2	1.0	1.0	1.0	1.0	
	R3	0.974	0.934	0.975	0.979	
	R4	0.765	0.711	0.817	0.719	
Normal Force Trailing Edge flap	R1	0.831	0.637	1.141	1.063	Pitch due to Left & Right side I/B & O/B Flap deflection
	R2	1.0	1.0	1.0	1.0	
	R3	0.777	0.701	0.785	1.07	
	R4	0.438	0.417	0.227	1.02	
Roll Damping	R1	0.971	0.846	0.949	0.871	Pitch due to steady a/c roll Roll due to steady a/c roll rate
	R2	1.0	1.0	1.0	1.0	
	R3	0.456	0.421	0.777	0.846	
	R4	0.286	0.378	0.399	0.828	

Figure 28 shows the sensitivities versus Mach number for different flap maneuvers. It can be concluded from this figure that large differences exists in subsonic flight regime, whereas in the supersonic regime all sensitivities are converge to an asymptotic value at high supersonic speed. Similar to this example for all harmonization candidates the sensitivity has to be calculated, corrected with the mean value correction terms and packed into matrix form for the look up tables.

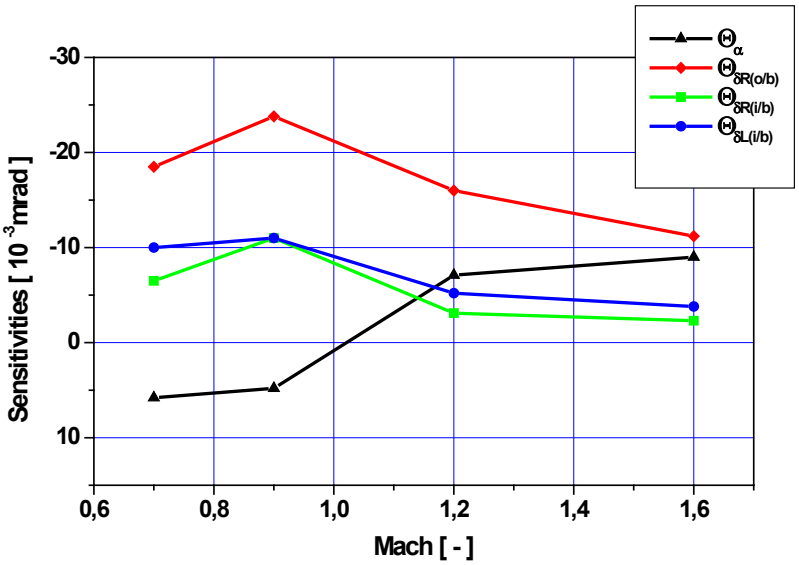

Figure 28: Sensitivity versus Mach number for stub pylon.

5.6 Deformations

The corrected sensitivities are the basis for determination of the deformations onboard during combat flight. Due to the high sophisticated flight control system the aircraft can be flown in carefree handling mode. This mode allows the pilot to fly the A/C in every possible maneuver, because the limiting load function of the FCS controls the A/C in that way that no load exceedance can be happen. For validation single maneuver are used, like the well-known MIL-standard maneuvers.

In Figure 29 the total deformation on the wing stub pylon is shown for different Mach number. The applied maneuver was a pull push maneuver.

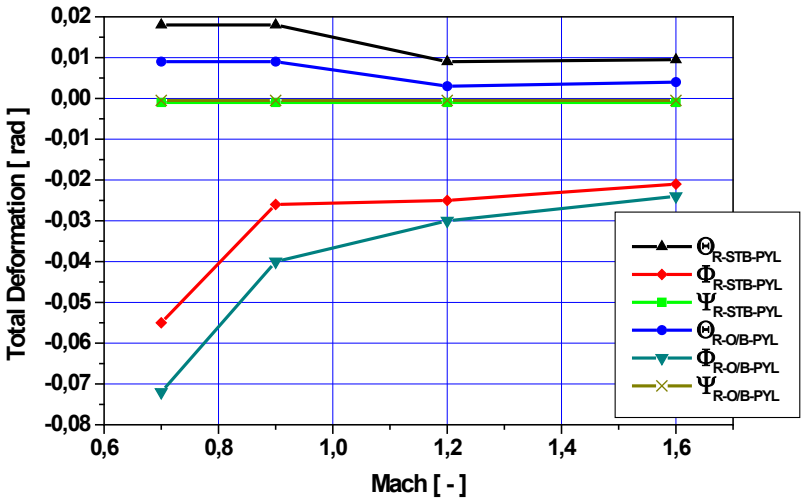

Figure 29: Total Deformation vs. Mach number.

5.7 Validation

Before the aircraft will be flight tested, the procedure must be validated. In the first step the deformation can be checked with some results from Major Airframe Static Test (MAST). During this test the airframe structure is penetrated with different loads stemming from extreme maneuvers. This test is required to prove that the airframe can withstand the loads produced by extreme maneuvers. For known single maneuvers, the measured deflection on the wing can be used for comparison with the analytical results from harmonization process.

	MAST	HARMONISATION
• rapid roll	-10.4 mrad	-12.0 mrad
• pull	-50.9 mrad	-52.0 mrad

The numbers show good correlation between the measurement on MAST and via Harmonization analysis.

In the next step, the deformation should be measured during flight test.

5.8 Grouping of Different Stores

During development of this harmonization procedure it turned that a large number of configuration have to be investigated to cover all pointing errors of the selected candidates. In the first approach each possible configuration was investigated, because no experience about the different stores was available and to establish a database for further investigation. Also different fuel states were introduced as new configurations. In the end of the analysis the large amount of results have to be reduced due to the limited available space in the weapon computer for look up tables. To keep the look up table in the agreed size a procedure have to be found where stores with similar dynamic behavior in view of pointing error can be packed together. An example is shown in Figure 30. The criterion was defined as 6 mrad. This is a useful number, because is describe in general the tolerances inside the Avionic for this kind of processes.

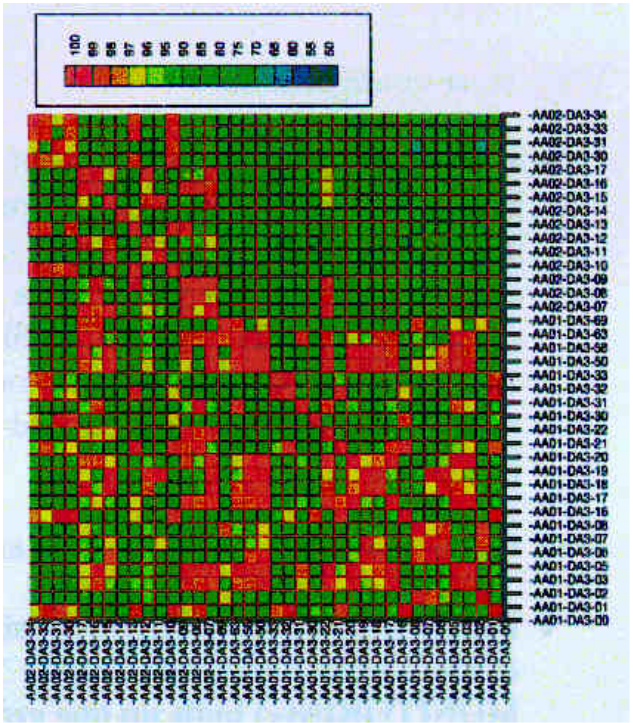

Figure 30: Grouping Matrix.

This figure describes in matrix form the correlation between different store configurations. The dark color describes a very good correlation by applying the 6 mrad criterion. This matrix should be symmetric, but that only one side of the aircraft was set as a fixed reference, only the lower triangular matrix describes the grouping well.

5.9 Conclusion – Store Pointing Error

A modal based procedure for store harmonization algorithm has been developed static aeroelastic constraint analysis. The method is based on using unit load cases in combination to evaluate overall flexible aircraft deformations.

This modal approach analysis show satisfactory correspondence to static aeroelastic approach. The modal analysis approach was chosen, because all required unsteady aerodynamic data was available from other structural dynamics investigations.

A grouping process for the different store configurations was required due to the limitation of the available size of the look up tables.

In the first step, the procedure has been compared with the deformations derived from Major Airframe Static Test. The results show good correlation between test and analysis. In the next step a validation of the calculated deformation of the selected harmonization candidates will be done by flight testing.

6.0 LOCAL AIRCRAFT STRUCTURAL DEFORMATION DUE TO EXTERNAL STORE CARRIAGE

The state of the art analysis of the separation behaviour of an external store doesn't consider the effects of local structural deformations of the carriage devices and launch equipment.

Such deformations may be caused by steady/unsteady inertia and aerodynamic loads. The order of magnitude of such deformations ranges between negligible and up to considerable values of several degree. If neglected within the prediction of separation behaviour, a consecutive flight test result normally comes up with bad evidence.

Time accurate representations of the 6 degree of freedom motions simultaneously and reciprocally interacting with the complex flow architecture around a separating store and the releasing aircraft should be taken into account of the analysis. Viscous flow effects as well as the global representation of flows with multiple phases should be introduced to the long term goals of future efforts.

Structural interactions between store and aircraft are very well handled as far as flutter, vibration and acoustics are concerned, but still remain a progressive area for future engineering tasks concerning store separation.

In this context, Deformation shall be understood as a quasi-steady state continuous response of the aircraft structure and the carriage equipment which are reacting to the forces and moments implemented by the inertia loads of the store in connection with the manoeuvre loads of the aircraft in addition to the resulting interference aerodynamic loads acting on the store:

- Heavy stores are mostly exposed to such effects, as well as stores with distinct aerodynamic characteristics. Light weight stores with slender bodies are not potential candidates but can be involved by second line effects.
- Asymmetric installation positions, off the plane of symmetry of the aircraft, are mostly exposed to such effects. Wing stations are adequately affected.

Thereby structural deformation is primarily induced by the lateral forces and moments acting on the store attachment points. The contribution of axial force, lift and pitching moment can be considered as negligibly small.

If not taken into account when analytically predicting a separation process, the presence of structural deformation may considerably deteriorate the results expected from a comparative flight test case. Figure 31 illustrates such a situation, in which the rigidly computed trajectory clearly differs from the trajectory data gained from the analysis of the flight test results.

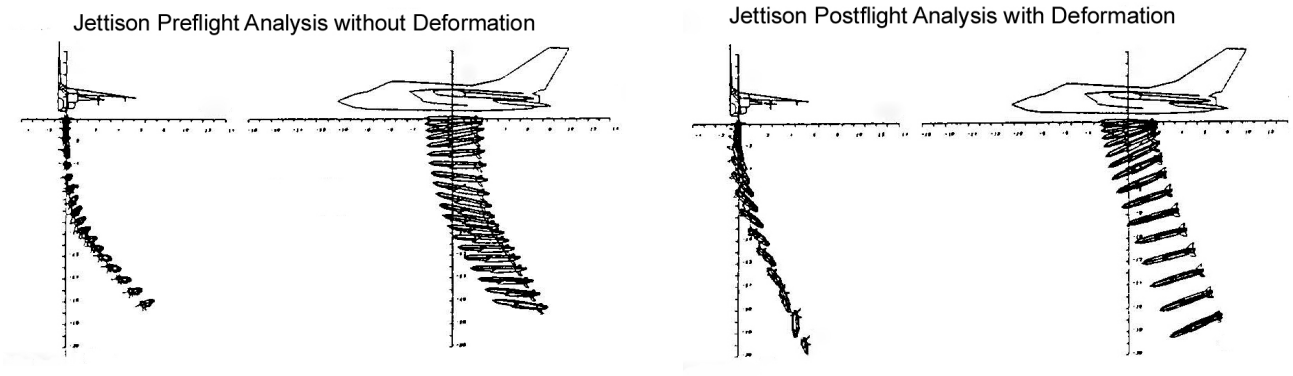

Figure 31: Jettison with and w/o deformation.

Taking into account the rigid installation position, the predicted store motion behaves quite neutral in roll after release, whereas a strong rolling motion with rates up to 150 °/s is indicated by the flight test data.

By introducing a small installed misalignment of less than 1° in roll and yaw, the computed results can be considerably improved such as to provide a perfect agreement with the data derived from flight test. As it will be shown in the following, this alignment error was in full agreement with in-flight deformation measurements which have been carried out in parallel to this jettison test.

The good agreement is documented by the comparisons shown in Figure 32 and 33 which represent the two Euler angles, pitch and yaw, taken from the experiment and the two computations with and without consideration of the contributions from structural deformation.

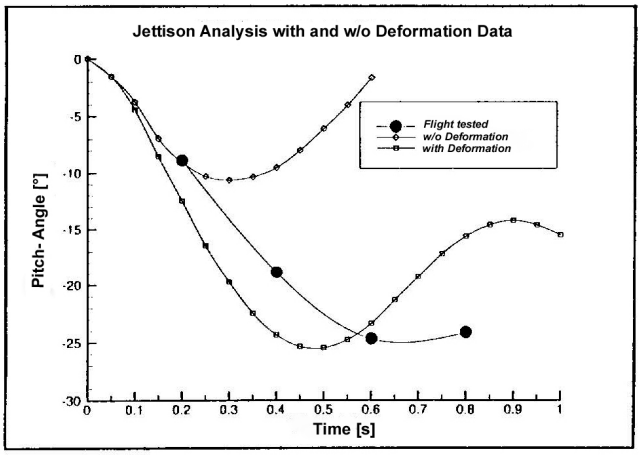

Figure 32: Jettison Analysis Pitch Angle.

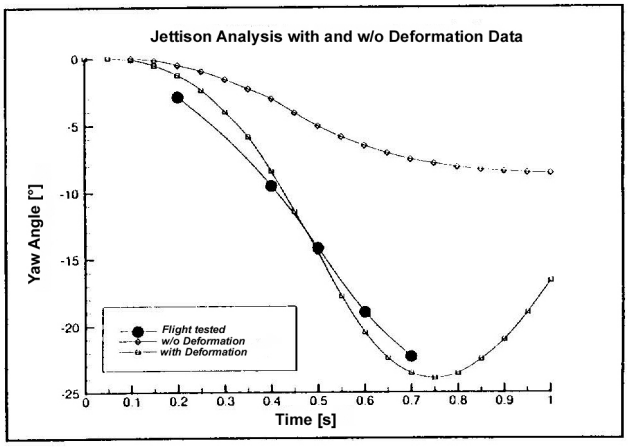

Figure 33: Jettison Yaw Angle.

These loads represent the rigid aircraft properties and do not include effects implemented by structural deformation arising from aeroelasticity or manoeuvring loads.

During the flight test data acquisition phase such effects can be assessed if the store attachment and carriage devices are properly instrumented and balanced. The flight tested sideforce coefficients have been assessed from records taken during wind-up turns for a >8° and roller- coaster manoeuvres for a <10° at minimised sideslip angles. The difference between flight test and wind tunnel coefficients is a clear indication for the presence of a steady state structural deformation as described in the preceding chapter. It varies for each flight test condition and also strongly responds to the load factor levels. The characteristic is strongly non-linear with respect to the effective angle of attack. It is also remarkable that at a. >8° the sideforce gradient is inverted against the trend measured in the wind tunnel.

As far as safe separation is concerned, it is not sufficient only to implement some correction loads to the installed loads in order to get the full story. In addition to this it is also necessary to specify the incremental alignment induced by the deformation, in order to provide the full description of the initial condition into the separation code.

Any angular term in roll or yaw will contribute additional terms to the release disturbance and thus change the motion of the store after release.

Bearing in mind that such deformations are quite inaccessible to theoretical analysis, the determination of these misalignments remains a main objective of further experimental efforts. A pragmatic approach to this purpose consists in using a ground-stiffness test involving a store installed to the aircraft. The general test arrangement therefore is shown in Figure 34, where one can see how the hydraulic actuator is operated in order to generate predefined loads on the store installed to the aircraft. Two actuators are used one at each end of the store such as to generate symmetric and antimetric forces and moments. Figure 35 shows the sensors installed to the different areas in which the deformations had to be recorded. Typical results are shown in Figure 36, where the measured deformations are plotted against the applied total yawing moment. These functions are assessed at the nose and for the rear part of the store and have a non-linear character due to the backlash of the attachment mechanism.

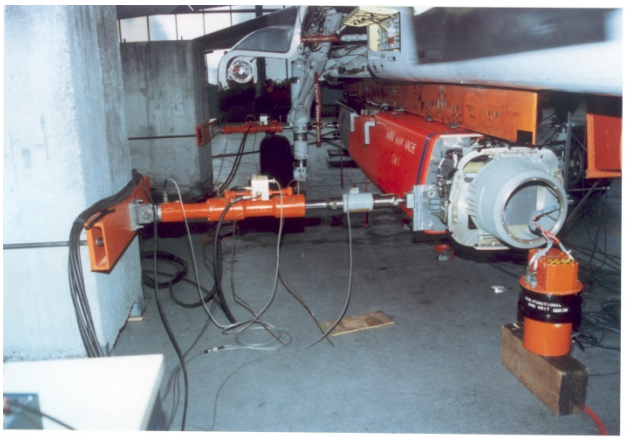

Figure 34: Stiffness Test detail.

Figure 35: Stiffness Test under fuselage Store.

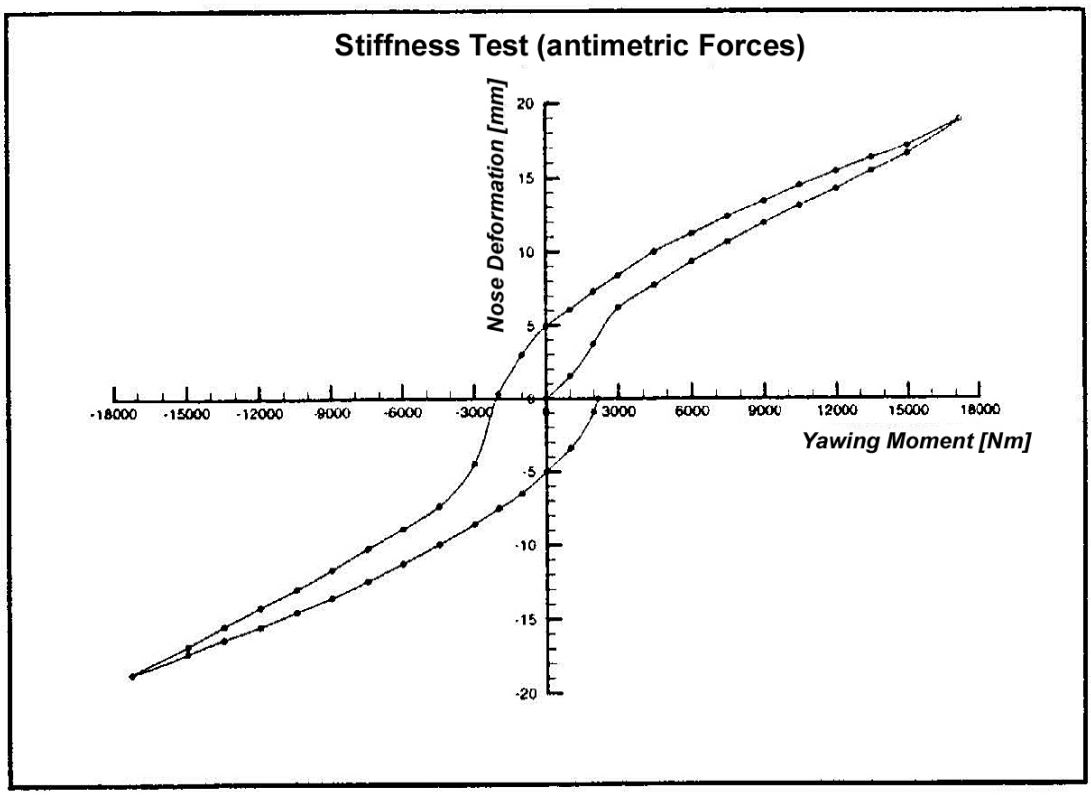

Figure 36: Deformation Measurement – Nonlinear behaviour.

Nowadays structural deformation must be considered as an important contribution for a store separation analysis. If not taken into account, the deformation terms easily can deteriorate the matching process by initiating misleading corrections to a dataset. The risk of a separation hazard for the affected store types is considered as low, however misinterpreted corrections may result in too pessimistic limitations for the separation envelope. Especially for guided release or auto-piloted separation this knowledge is essential for a proper design process of the flight control system. Although inaccessible to theory several experimental approaches and concepts provide reasonable methods for its quantification.

7.0 ACOUSTIC LOADS

7.1 Influence of Acoustic Loading on Supersonic Fuel Tank

The supersonic fuel Tank is mounted on the centre wing or the centre fuselage station on combat Aircraft. Cracks were detected on the flat panels of the integrated pylon, Figure 37. Additionally internal cracks on flanges were identified and equipment fittings failed. The probable reasons for this damage are the dynamic stimulation by high acoustic loading of the flat panels and the subsequent severe vibration.

Figure 37: Cracks between tank and integrated pylon and on integrated pylon panels (tried to repair by tape).

Aerodynamic noise from the wing, fuselage and tank and cavity noise from the main undercarriage bays can be responsible for these kinds of damages.

Cavity noise has been measured in the Combat Military Aircraft main undercarriage bays on different Airplanes, with one microphone. Flight test measurements were evaluated to demonstrate the influence of extended and retracted undercarriage on the Overall Sound Pressure Level (OASPL) in relation to velocity, the result is shown in Figure 38. Due to cavity noise the OASPL's in the opened main undercarriage bay increase significantly up to 145 dB with max. allowable velocity. The maximum velocities of the operating and extended undercarriage are defined in the "Structural Design Criteria Production".

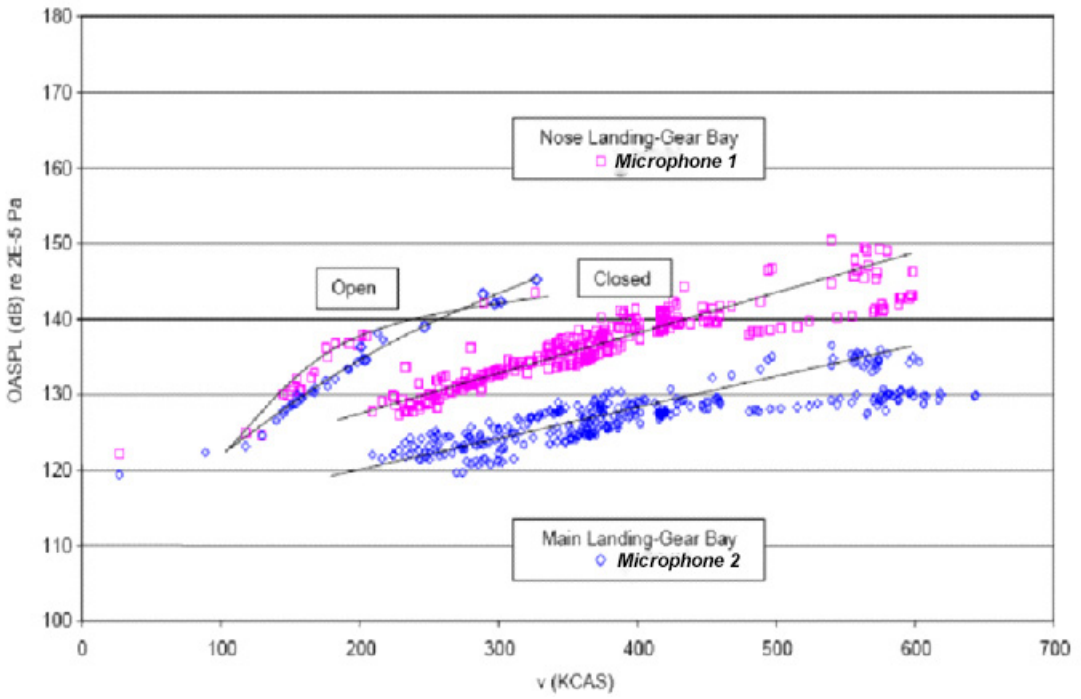

Figure 38: OASPL in opened and closed nose and main undercarriage bays in relation to velocity.

The flat panels of the integrated pylon can also be stimulated by aerodynamic noise. Unfortunately no pressure sensors were installed on the wing and fuselage pylons. From Tornado flight test data it is known that OASPL >170 dB occur on the panels of the I/B pylon in the transonic regime, Figure 39.

Figure 39: Location of Acoustic Sensors on Tornado I/B Pylon with Tank and Stub Pylon.

Additionally in the extended undercarriage configuration the distance of 1 inch between main undercarriage doors and Supersonic Fuel Tank on centre fuselage station can generate severe acoustic loading on the integrated pylon.

For the investigation of the SFT structural damages it is proposed to analyse the acoustic fatigue life of the critical pylon panels and flanges with the Tornado pylon acoustic loading spectrum and the flight test results of the tested Aircraft main undercarriage cavity noise measurements.

8.0 REFERENCES

1) Luber W., Becker J., Sensburg O.
Impact of Dynamic Loads on the Design on European fighter
43rd Structures and Material Panel Conference, AGARD Florence 1996.

2) Becker J., Dau K.
Evaluation of vibration levels at the pilot seat caused by wing flow separation.
44th Structures and Materials Panel of AGARD, Lisboa, April 1977.

3) Luber W., Becker J.
Comparison of Piezoelectric Systems and Aerodynamic Systems for aircraft Vibration Alleviation
SPIE's 5th Annual International Symposium on Smart Structures and Materials, Conference 3326,
March 1998, San Diego, USA.

4) Becker J., Luber W.
The Role of Buffet in the Design of European Fighter
44th AIAA Structural and Materials Conference
April 2003, Hampton, USA.

5) Deslandes R.
Structural Deformation – A New Challenge to the Accuracy of Separation Codes
RTO-SCI Symposium Chester, United Kingdom, 1998.

6) Luber W., Hafner M.
Calculation of Store Pointing Error due to Flexible Aircraft under Load
International Forum of Aeroelasticity and Structural Dynamics, Madrid, Spain, 2001.

7) Harris Cyril M.
Shock and Vibration Handbook
McGraw-Hill Book Company.